SCIENTIFIC REPORTS

OPEN

SUBJECT AREAS:
NANOWIRES
SYNTHESIS AND PROCESSING

Received
19 November 2014

Accepted
7 January 2015

Published
30 January 2015

Correspondence and requests for materials should be addressed to Y.L. (liuyong7@mail.sysu.edu.cn)

Confined-space synthesis of single crystal TiO_2 nanowires in atmospheric vessel at low temperature: a generalized approach

Xiaoyue Wang[1,3], Hai Wang[2], Yu Zhou[1], Yong Liu[1], Baojun Li[1], Xiang Zhou[1] & Hui Shen[1]

[1]School of Physics and Engineering, State Key Laboratory of Optoelectronic Materials and Technologies, Sun Yat-sen University, Guangzhou 510275, China, [2]Key Laboratory of New Processing Technology for Nonferrous Metal and Materials, Ministry of Education, Guilin University of Technology, Guilin 541004, China, [3]Department of Materials Science and Engineering, McMaster University, Hamilton, Ontario, Canada.

Extensive efforts have been devoted to develop innovative synthesis strategies for nanomaterials in order to exploit the true potential of nanotechnology. However, most approaches require high temperature or high pressure to favor crystallization. Here we highlight an unconventional approach for the confined-space synthesis of the single crystal TiO_2 nanowires in the atmospheric vessel at low temperature by cleverly manipulating the unique physical properties of straight-chain saturated fatty acids. Our method also applys to icosane due to its straight-chain saturated hydrocarbon structure and similar physical properties to the saturated fatty acids. Interestingly, we also found that the unsaturated fatty acids can facilitate the crystal growth, but their bent chains lead to the formation of TiO_2 particle aggregates. In addition, we demonstrate the growth of TiO_2 nanowires on arbitrary substrates, which are of great importance for their wider applications. We thus anticipate our presented method to be a possible starting point for non-classical crystallization strategies and be easily adapted for the fabrication of all other inorganic materials.

The search for cheap, efficient, and novel nanomaterial fabrication technology has been motivated intensively in various fields of nanotechnology. TiO_2 has been extensively investigated as a key semiconductor material in water photosplitting, photocatalyst, lithium-ion batteries, gas sensor, and photovoltaic cells due to its excellent properties, low cost, environmental friendliness, and the fact that it is widely available[1–6]. The ability to grow oriented single crystal TiO_2 nanowire/nanorod arrays is highly desirable for above applications because of their superior photoelectronic properties[7–11]. To date, the most effective strategies involve the template-assisted electrodeposition route[12], chemical vapor deposition[13,14], and hydrothermal/solvothermal methods[11,15–25]. However, these approaches are not very ideal considering their following disadvantages. For example, chemical vapor deposition method needs high temperature reactions, high energy cost, and has low productivity. The template-assisted electrodeposition route needs complex and tedious multi-step procedures involving the preparation of anodic aluminum oxide (AAO) template, electrodepostion, and removal of AAO template. In addition, heat treatment is also required for the amorphous to crystalline phase transformation. The hydrothermal/solvothermal synthesis are normally performed in high-pressure stainless steel vessel called an autoclave since they are usually conducted under a temperature higher than the boiling temperature of the solvent, which limit their safety and large-scale production. Furthermore, for the typical hydrothermal synthesis of TiO_2 nanowires, the use of high concentration of strong alkaline (*e.g.* sodium hydroxide)[15,16] or strong acid (*e.g.* hydrochloric acid)[11,18–25] can cause corrosion of equipment and the industrial waste discharge. Therefore, it is highly desirable to develop simple, low cost, high yield, and environmentally friendly synthesis methods for direct fabrication of oriented single crystal TiO_2 nanowire arrays at low temperature and preferably under atmospheric conditions.

Results

Here we present for the first time a unified approach for the confined-space growth of the single crystal TiO_2 nanowires using the saturated fatty acids such as lauric acid ($C_{12}H_{24}O_2$), myristic acid ($C_{14}H_{28}O_2$), palmitic acid ($C_{16}H_{32}O_2$), and stearic acid ($C_{18}H_{36}O_2$). The pictured fabrication process for the TiO_2 nanowires can be readily

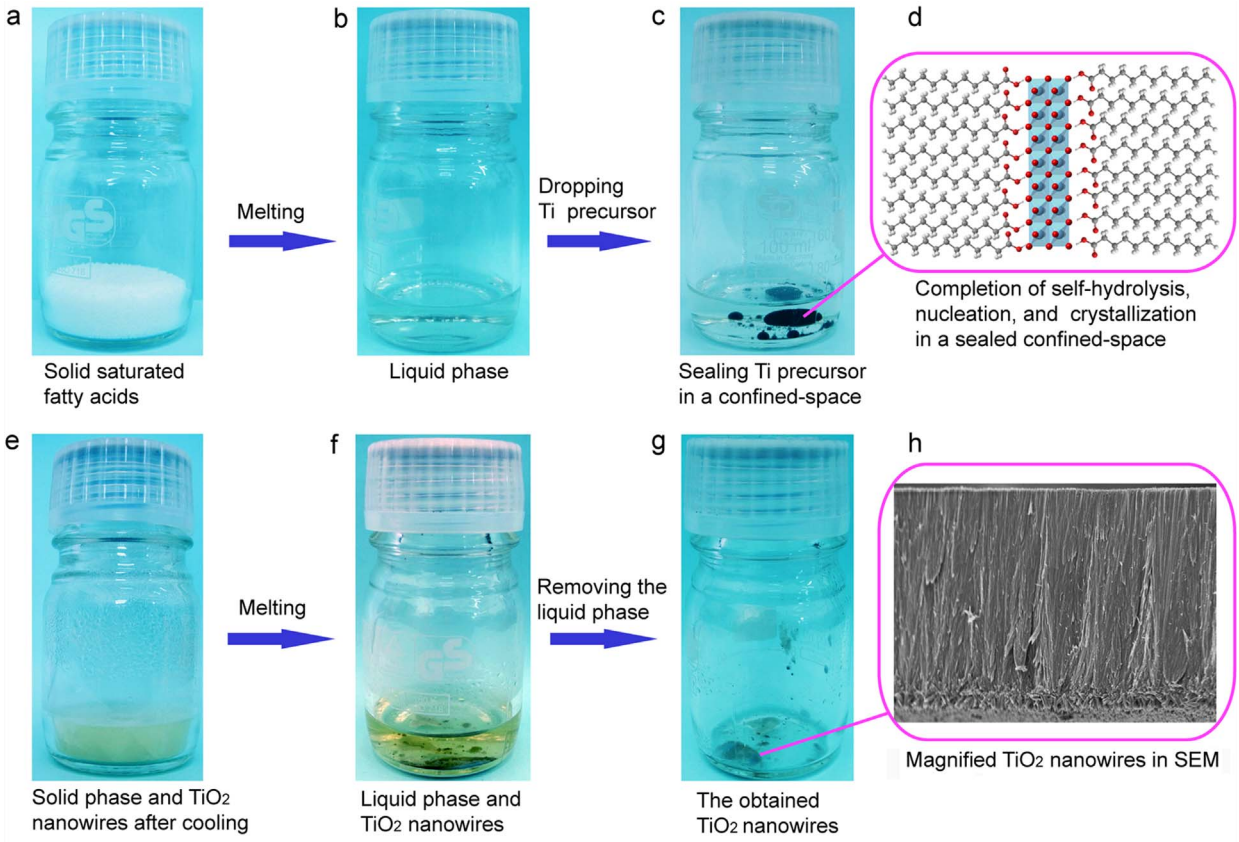

Figure 1 | Schematic illustration for the confined-space synthesis of TiO_2 nanowires in atmospheric glass vessel at low temperature.

seen in Fig. 1. The salient features of our synthesis strategy is that well crystal TiO_2 nanowire structures can be easily fabricated in atmospheric glass vessel at low temperature by cleverly manipulating the unique physical properties of saturated fatty acids (Supplementary Table S1). Taking lauric acid as an example, firstly, its melting point must be very low (*e.g.* 44°C) so that we can melt the solid saturated fatty acids into liquid phase easily, and more importantly, the hydrolysis of dropped Ti precursor can be avoided at such low temperature. Secondly, its density (*e.g.* 862 kg/m^3) is necessary to be lower than the aqueous $TiCl_3$ solution so as to float on the top of the aqueous $TiCl_3$ solution. Thirdly, it must be water-insoluble so as to form liquid-liquid interface with the aqueous $TiCl_3$ solution. Fourthly, the boiling temperature (*e.g.* 298.9°C) should be much higher than the reaction temperature (60–150°C) so that melted fatty acids can form the stable sealing layer to confine the produced water vapor around aqueous $TiCl_3$ solution during the reaction. And then self-hydrolysis of the aqueous $TiCl_3$ solution, TiO_2 nucleation, and subsequent crystallization can be realized in such sealed confined-space. Finally, saturated fatty acids should have straight chains, and their molecules can be packed together very tightly, allowing TiO_2 nuclei to grow within the saturated acid matrix and fused together into one-dimensional structures. Therefore, the saturated fatty acid plays a dual role in above TiO_2 nanowire synthesis: on the one hand, it forms a "soft" sealing layer to confine the water vapor around the $TiCl_3$ solution and then produce enough pressure to favor crystallization in this small confined space. On the other, it also acts as a soft template to induce the formation of one-dimensional structure. Therefore, our unique methods are different from the conventional approaches such as traditional calcination, chemical vapor deposition, and hydrothermal methods which require high temperature treatment or high pressure vessel to complete crystallization.

Figure 2 shows field emission scanning electron microscopy (FESEM) images of products fabricated by using different saturated fatty acids such as lauric acid (Fig. 2a and b), myristic acid (Fig. 2c and d), palmitic acid (Fig. 2e and f), and stearic acid (Fig. 2g and h), respectively. As expected, all the samples show morphologies of highly oriented TiO_2 nanowire array since these saturated fatty acids have similar physical properties as described in Supplementary Table S1. Figure 2a, c, e, and g are side view FESEM images of highly oriented TiO_2 nanowire arrays, and the length of the oriented nanowire arrays is ranging from 3 to 6 μm. Figure 2b, d, f, and h are top view of the same samples, showing that the film is composed of uniform and well-separated nanowires. Figure 3 shows the X-ray diffraction (XRD) patterns of all above samples, and all the diffraction peaks match well with those of the tetragonal rutile TiO_2 phase (JCPDS no. 75–1750).

Lauric acid was chosen as an example to synthesize TiO_2 nanowires for further investigation of their characteristics and properties. Figure 4 shows transmission electron microscopy (TEM) image, selected area electron diffraction (SAED), and high resolution TEM image of as-prepared TiO_2 nanowires. SAED confirms that TiO_2 nanowires have the single crystal rutile structure (Fig. 4a). It is obtained from Fig. 4b that the diameter of nanowires is about 10 nm. Moreover, the distance between the adjacent lattice fringes is 0.325 nm, which can be assigned to the interplane distance of the rutile TiO_2 (110) plane. The angle between the (110) plane and the growth direction [001] was measured to be 90°, indicating that the growth direction of the TiO_2 nanowires is along the [001] direction.

The TiO_2 nanowires show a type IV isotherm with H3 hysteresis loop (Supplementary Fig. S1), which implies the existence of mesopores (2–50 nm). The pore size distribution was derived from the desorption branches of the isotherms using the Barrett-Joyner-Halenda (BJH) method (the inset in Supplementary Fig. S1). The corresponding pore size peak is 1.59, 2.73, 3.43, 6.85 and 8.63 nm, respectively, indicating the highly mesoporous nature of the TiO_2 nanowires. As calculated by the Brunauer-Emmett-Teller (BET)

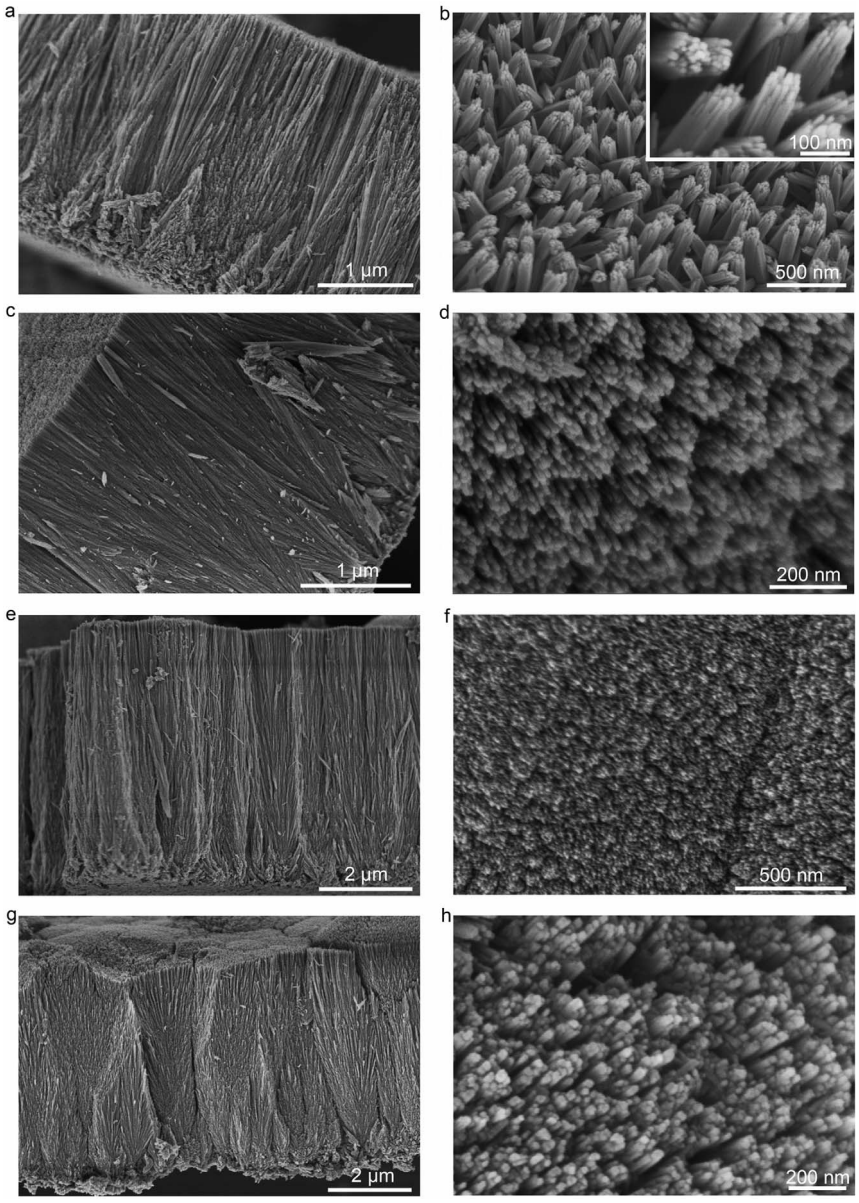

Figure 2 | FESEM images of the as-synthesized TiO_2 nanowires grown in atmospheric glass vessel by using 0.3 mL of $TiCl_3$ solution and 15 g of different saturated fatty acids at 150°C for 12 h. (a) and (b) lauric acid, (c) and (d) myristic acid, (e) and (f) palmitic acid, (g) and (h) stearic acid.

method, such porous structures give rise to a high specific surface area of 60.6 m^2 g^{-1}. The thermal gravimetric analysis (TGA) were used to investigate the residual organic species existed in mesoporous structure of nanowires, as shown in Supplementary Fig. S2. The as-prepared sample contains only 7 wt% of organic species, and the weight loss of 1.5 wt% around 100°C can be attributed to the evaporation of adsorbed moisture. Since the amount of residual organic species in nanowires is very small, we inferred that the formation of the mesoporous structure is attributed to the void of inter-nanowires instead of residual lauric acid.

To investigate the formation process of the TiO_2 nanowires, time-dependent experiments were carried out, as shown in Supplementary Fig. S3. The morphology of products collected at early stage exhibited separated flower-like nanowire aggregates with a diameter of about 1.5 μm after 1 h of reaction (Supplementary Fig. S3a). Interestingly, prolonging the growth time to 2 h, these flowers were bound together and had a tendency to form oriented nanowire thin film (Supplementary Fig. S3b). As the reaction proceeded to 3 h, the ordered degree of nanowires increased further (Supplementary Fig. S3c). With an increase of reaction time up to 6 h, the oriented TiO_2 nanowire arrays were finally formed (Supplementary Fig. S3d). When the growth time was further extended to over 12 h, the length and orientation of the TiO_2 nanowire arrays were identical without any change (Fig. 2a). At that time, the total reaction reached the equilibrium.

Supplementary Figure S4 shows the SEM images of the products after reaction of 0.3 mL of $TiCl_3$ precursor in 15 g of Lauric acid for 12 h at temperatures varying from 60°C to 120°C. At lower temperature of 60°C and 80°C, nanowire aggregates accompanied by many nanodots began to form (Supplementary Fig. S4a, b). When increasing the temperature to 100°C, the fully well separated nanowires were formed through the Ostward ripening process[26], and the accompanying nanodots began to disappear (Supplementary Fig. S4c). When the temperature was further increased to 120°C, oriented nanowire arrays formed (Supplementary Fig. S4d). Similar to the time dependent experiments, there were almost no changes of the length and orientation of the TiO_2 nanowire arrays while the reaction temperature was further increased up to 150°C (Fig. 2a).

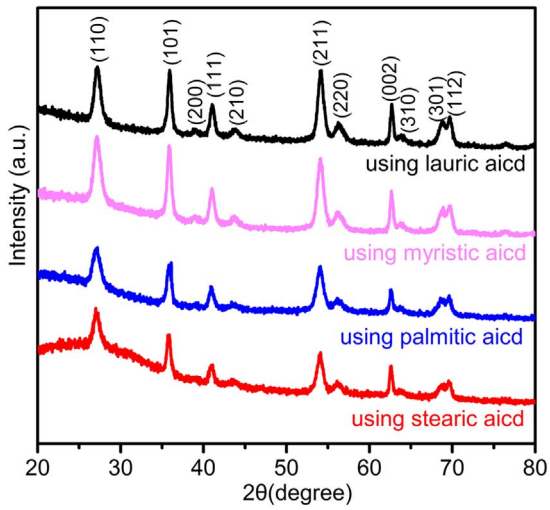

Figure 3 | XRD pattern of the TiO_2 nanowires fabricated in atmospheric glass vessel by using different saturated fatty acids at 150°C for 12 h.

We have also investigated the effect of various concentration of $TiCl_3$ solution on the formation of TiO_2 nanowire film. While the concentration of $TiCl_3$ solution decreased from 9% to 6%, and to 3%, the TiO_2 nanowire array films were still obtained (Supplementary Fig. S5a, b, and c). With further decrease of the concentration to 1%, only small amount of TiO_2 nanowires formed on the partial area of film (Supplementary Fig. S5d). Therefore, the nanowire growth kinetics is also possibly governed by the concentration of $TiCl_3$ solution, and the low concentration of $TiCl_3$ solution can increase their partial vapor pressure and evaporation rate. The fast evaporation caused relatively low pressure around the $TiCl_3$ solution, which is unfavorable to the formation of nanowires. To investigate the relations between the evaporation rate and the confined vapor pressure around $TiCl_3$ solution, we added the 15 g and 50 g lauric acid in the vessel without lid to seal $TiCl_3$ solution, respectively. By adding 15 g lauric acid and with lid off, only irregular shaped structures were produced. We noticed that there are untrafine vapor bubbles around $TiCl_3$ solution. These bubbles might slowly push their way out of the lauric acid and into the atmosphere, leading to relatively low pressure around $TiCl_3$ solution, which is unfavorable to the TiO_2 nanowire formation. In the our original experiments, with the lid on and 15 g lauric acid added, even small amount of vapor escaped from the sealing layer, but they could be confined in the upper space of the vessel by the lid, which would increase the pressure above lauric acid. Therefore, most of the vapor molecules colliding with lauric acid would not have sufficient kinetic energy to overcome this soft sealing layer and they would stick to the surrounding area of $TiCl_3$ solution, thereby, the evaporation rate with lid is much slower than that without the lid, which would produce high pressure in small area around $TiCl_3$ solution and thereby favor the formation of TiO_2 nanowires. Remarkably, when the amount of lauric acid increased to 50 g, even with the lid off, the soft sealing layer was thick enough to confine vapor molecules around $TiCl_3$ solution, which has the same effects as conditions with lid on and 15 g lauric acid added. As shown in Supplementary Fig. S6, well crystallized TiO_2 nanowire film was obtained.

Considering the potential application in future, we also designed the following experiments. Firstly, our method only utilizes the physical properties of saturated fatty acid instead of chemical reaction to favor the formation of nanowires. From point of economic view, we also recycled the previously used lauric acids and covered onto fresh $TiCl_3$ solution to grow nanowires in the vessel. Amazingly, perfect TiO_2 nanowire film can also be grown by using the recycled lauric acid (Supplementary Fig. S7). Secondly, we added much more $TiCl_3$ solution in the same vessel to grow nanowires, and then the TiO_2 nanowrie production and film thickness increased accordingly. As shown in Supplementary Fig. S8, the mass of obtained film is 0.026 g, 0.065 g, 0.194 g, and 0.239 g after 0.3 mL, 1 mL, 3 mL, and 5 mL $TiCl_3$ solution reacted in the vessel, respectively. In addition, the thickness TiO_2 nanowire film is up to 35 μm while the 5 mL of $TiCl_3$ solution was added (Supplementary Fig. S9).

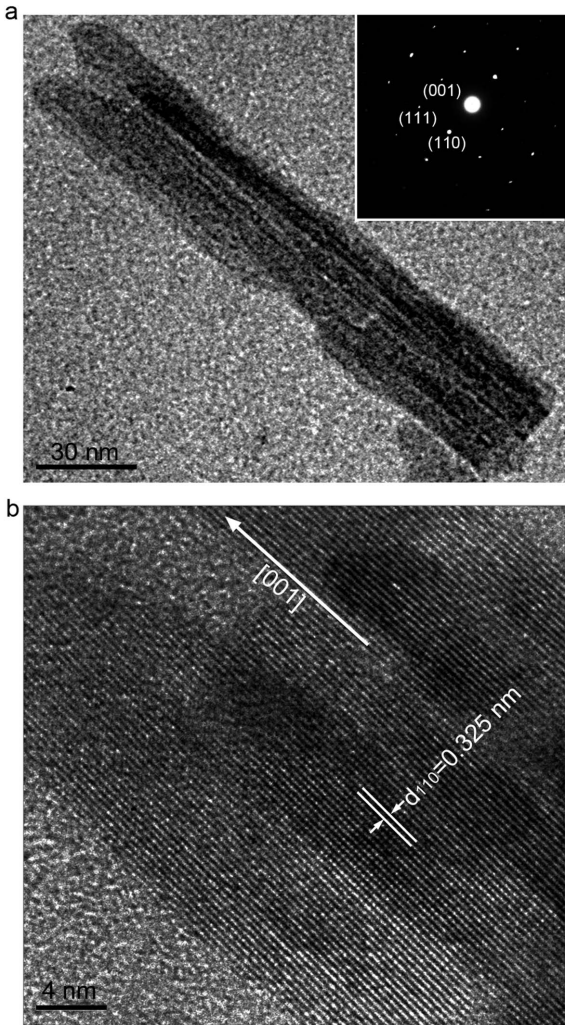

Figure 4 | Representative TEM results of TiO_2 nanowires produced with 0.3 mL of $TiCl_3$ solution and 15 g of lauric acid in atmospheric glass vessel at 150°C for 12 h. (a) TEM image and corresponding SAEDs of nanowires. (b) HRTEM image of the TiO_2 nanowires.

The above-mentioned TiO_2 nanowire structures can also be synthesized on arbitrary substrates such as silicon substrate, fluorine doped tin oxide (FTO) glass, Ti foil, and Teflon substrate. As shown in Fig. 5a and b, hierarchical TiO_2 microspheres assembled from oriented nanowires were formed on silicon substrate. In addition, the oriented TiO_2 nanowire arrays can also be grown on FTO glass substrate coated with thin TiO_2 seed layer (Fig. 5c), which is similar to that fabricated by using hydrochloric acid assisted hydrothermal method[18]. While this synthetic method was applicable to the Ti foil, flower-like nanowire aggregates were formed (Fig. 5d, e). Interestingly, a two-side oriented nanowire arrays can be produced on Teflon substrate (Fig. 5f), which was similar to that obtained by reacting titanium powder with a mixture solution of H_2O_2 and HCl under hydrothermal condition[27]. The different morphology of nanowire aggregates formed on arbitrary substrates are due to the different surface property of the substrates, which are also of great importance to nanowires in wider application such as water photosplitting, photocatalyst, gas sensor, and photovoltaics.

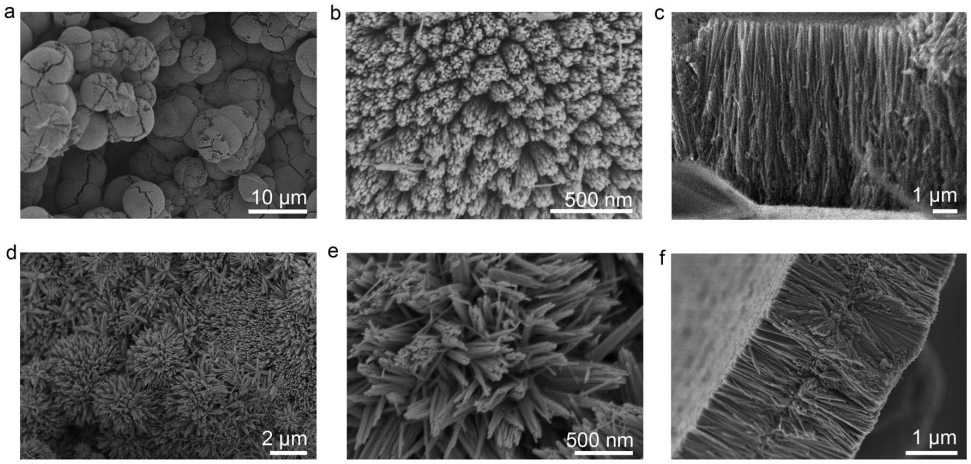

Figure 5 | Confined synthesis of TiO_2 nanowires on arbitrary substrates by using 0.3 mL of $TiCl_3$ solution and 15 g of lauric acid in atmospheric glass vessel at 150°C for 12 h. (a) and (b) silicon substrate, (c) FTO glass, (d) and (e) Ti foil, (f) Teflon substrate.

Discussion

As we described before, the confined growth of the single crystal TiO_2 nanowires are conducted by using the saturated fatty acids such as lauric acid, myristic acid, palmitic acid, and stearic acid, which is different from the conventional hydrothermal method. Then, there are three issues need to be addressed. One is why the TiO_2 nanowires possess rutile structure instead of anatase structure. The second question then arises what is the underlying factor that affects the formation of nanowire structures, and whether unsaturated fatty acids (*e.g.* oleic acid) can give rise to the same results since they also have the similar physical properties with the above saturated fatty acids? The third issue is why the low reaction temperature can lead to high crystallinity in atmospheric glass vessel. For the first issue, $TiCl_3$ solution can easily be hydrolyzed and oxidized to octahedral monomer ($[TiO(OH_2)_5]^{2+}$) (rutile nuclei)[28]. According to the crystal structure of anatase and rutile TiO_2, the rutile TiO_2 crystalline structure is the linear chains of TiO_6 octahedra by sharing equatorial edges, while anatase is the spiral chain of apical edge sharing TiO_6 octahedra. In the interfacial region of saturated fatty acid and $TiCl_3$ solution, linear chain arrangement of $[TiO(OH_2)_5]^{2+}$ octahedral monomers (rutile nuclei) can be easily shared equatorial edges than apical edge sharing spiral structures due to the geometric confinement of fatty acid molecular with similar line chain structure. For the second issue, the boiling temperature of oleic acid is 360°C (at 760 mmHg), in addition, it is water-insoluble and lighter than water (Supplementary Table S1), and it also seems to be suitable for growing TiO_2 products by our confined-space synthesis method in atmospheric glass vessel at low reaction temperature. To appreciate this, we also investigated the reaction of the $TiCl_3$ solution confined by oleic acid in atmospheric glass vessel at temperature of 150°C for 12 h. As we expected, the crystallization phase of obtained sample was also rutile (Fig. 6a). However, the as-prepared aggregates were distributed in random, as shown in Fig. 6b. Oleic acid is typical unsaturated fatty acid, therefore, we infer that the differences in geometry between saturated and unsaturated fatty acids play an important role in the construction of nanostructures. For saturated fatty acid, it is an amphiphilic linear monomer, containing a hydrophobic alkyl group ($-CH_3$) at one end, a long hydrocarbon chain, and a terminal carboxylate group (-COOH) at the other end. There are no double bonds between the carbon atoms in saturated fatty acid chain as the carbons are fully "saturated" with hydrogen atoms. As a result, saturated fatty acids form straight chains and can be packed together very tightly. In addition, $TiCl_3$ precursor itself contains an amount of water and the hydrolysis can easily occur. Accordingly, with the increase of temperature and time, TiO_2 nuclei can diffuse within the saturated fatty acid matrix and fuse together into the one-dimensional nanowires during

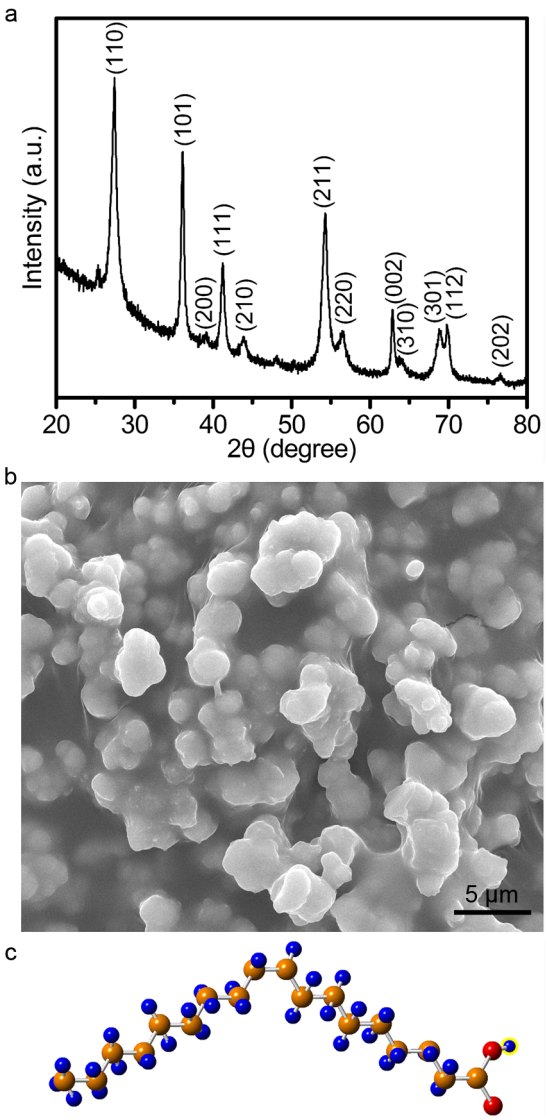

Figure 6 | The confined-synthesis of TiO_2 samples in 0.3 mL of $TiCl_3$ solution and 15 g of oleic acid in atmospheric glass vessel at 150°C for 12 h. (a) XRD measurement. (b) FESEM images. (c) Schematic illustration for molecular structure of oleic acid. Here, the yellow, blue, and red balls represent C, H, and O atoms, respectively.

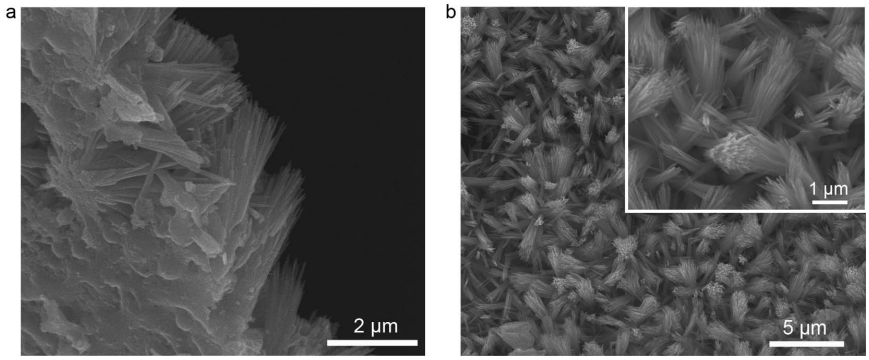

Figure 7 | The TiO_2 nanowire arrays obtained by using 15 g of icosane to confine 0.3 mL of $TiCl_3$ solution in atmospheric vessel at 150°C for 12 h. (a) Cross-sectional FESEM images of the TiO_2 nanowire arrays. (b) Top view FESEM images of the TiO_2 nanowire arrays. The inset is corresponding high magnification FESEM image.

the continuous reaction process. However, Oleic acid (18 : 1 n−9) has 18 carbon atoms with the first double bond occurring at the ninth carbon atom away from the carboxylic acid group, and thus creating bent chains (Fig. 6c). Therefore, their molecules cannot be packed tightly together, and the formed TiO_2 products are particle aggregates. For the third issue, both the saturated fatty acid and unsaturated acid can play a role of "soft" sealing layer to confine the water vapor around the $TiCl_3$ solution and then produce enough pressure to favor crystallization in the small confined space. However, their different is that saturated fatty acid with straight line chains also acts as a soft template to induce the formation of one-dimensional structure. The same concepts can also be applied to icosane ($CH_3(CH_2)_{18}CH_3$) in our method by considering its straight-chain saturated hydrocarbon structure and similar physical properties to saturated fatty acids (Supplementary Table S1). As shown in Figure 7, the TiO_2 nanowire arrays were also obtained by using icosane as soft sealing layer to confine the $TiCl_3$ solution.

Conclusions

In summary, we have presented for the first time the confined-space synthesis of oriented single crystal TiO_2 nanowires in atmospheric glass vessel at low temperature by cleverly manipulating the unique physical properties of saturated fatty acids and icosane. Moreover, the synthetic methodology we have developed is scalable, long-chain saturated fatty acids or n-alkane, such as lauric acid, myristic acid, palmitic acid, and stearic acid, and icosane, could provide a general confined-space strategy for the growth of TiO_2 nanowires in atmospheric glass vessel at low temperature. Our unique procedure is performed under mild conditions without the use of high temperature, high pressure vessel, and strong acids, thus saving energy and cost. In addition, we demonstrate the growth of TiO_2 nanowires on arbitrary substrates. We believe that these findings are of great importance for nanowires in wider applications. We found that the unsaturated fatty acids can also facilitate the crystallization of products, but their bent chains lead to the formation of TiO_2 particle aggregates. The unified approach strategies presented here are designed for TiO_2 materials but would be in fact general for all other inorganic materials. We thus anticipate our method to be a possible starting point for non-classical crystallization strategies and provide a new and deeper understanding of the crystal growth.

Methods

Sample preparation. In a typical synthesis, 15 g saturated fatty acids (*e.g.* lauric acid, myristic acid, palmitic acid, and stearic acid) were melted to form liquid phase in a glass vessel at 50–70°C. Then, 0.3 mL Titanium (III) chloride solution (≥12% $TiCl_3$ basis, 5–10% free aicd as HCl, Sigma-Aldrich) was dropped into the above melted acids. After that, the glass vessel was covered with the lid and kept at 150°C for 12 h for the confined-space synthesis of nanowires. Afterward, the glass vessel was taken out and cooled naturally to room temperature, and solid mixture of TiO_2 nanowire film and saturated fatty acids was obtained. Then the obtained mixture was heated at 70°C to melt the saturated fatty acids again. After the melted acids were removed, the nanowire films were collected, and washed with deionized water and ethanol for several times prior to be dried in air at 60°C. The growth temperature, reaction time, substrate, concentration and the amount of $TiCl_3$ solution, and other long-chain molecules (*i.g.* icosane, oleic aicd) were independently varied to investigate the effect of growth parameters on product formation according to above similar procedure. The $TiCl_3$ solution was diluted to 1-9% by using 10% hydrochloric acid aqueous solution to avoid hydrolysis. When more $TiCl_3$ solution was added (*e.g.* 1–5 mL), 50 g lauric acid was added to form the thick sealing layer to confine them in the vessel with the lid on.

Structural characterization. The surface morphologies of the samples were studied using FESEM (JEOL, JSM6300, Japan). The crystal structure was performed by XRD (PanAnalytic X'Pert Pro, Phillips) using Cu-Kα radiation (λ = 0.15405 nm, at 40 kV and 25 mA). The TEM, high-resolution TEM images, and SAED were obtained with a JEOL JEM- 2010F microscopy operating at 200 kV. Nitrogen adsorption-desorption isotherms were measured on a NOVA1200 instrument (Quantachrome Corporation) at 77 K. Prior to the measurement, the samples was degassed in a vacuum at 200°C for 12 h. The thermal properties of the samples were studied with thermogravimetric analysis (TG209, Netzsch Instruments, Germany) from 25 to 800°C.

1. Khan, S. U. M., Al-Shahry, M. & Ingler Jr, W. B. Efficient photochemical water splitting by a chemically modified n-TiO_2. *Science* **297**, 2243–2245 (2002).
2. Xing, J., Fang, W. Q., Zhao, H. J. & Yang, H. G. Inorganic photocatalysts for overall water splitting. *Chem. Asian J.* **7**, 642–657 (2012).
3. Nakata, K. & Fujishima, A. TiO_2 photocatalysis: design and applications. *J. Photochem. Photobiol. C: Photochem. Rev.* **13**, 169–189 (2012).
4. Zhu, G. N., Wang, Y. G. & Xia, Y. Y. Ti-based compounds as anode materials for Li-ion batteries. *Energy Environ. Sci.* **5**, 6652–6667 (2012).
5. Qiu, J. X., Zhang, S. Q. & Zhao, H. J. Recent applications of TiO_2 nanomaterials in chemical sensing in aqueous media. *Sensors and Actuators B* **160**, 875–890 (2011).
6. Bai, Y., Mora-Seró, I., De Angelis, F., Bisquert, J. & Wang P. Titanium dioxide nanomaterials for photovoltaic applications. *Chem. Rev.* **114**, 10095–10130 (2014).
7. Shankar, K. *et al.* Recent advances in the use of TiO_2 nanotube and nanowire arrays for oxidative photoelectrochemistry. *J. Phys. Chem. C* **113**, 6327–6359 (2009).
8. Han, B., Kim, S. J., Hwang, B. M., Kim, S. B. & Park, K. W. Single-crystalline rutile TiO_2 nanowires for improved lithium ion intercalation properties. *J. Power Sources* **222**, 225–229 (2013).
9. Arafat, M. M., Dinan, B., Akbar, S. A. & Haseeb, A. S. M. A. Gas sensors based on one dimensional nanostructured metal-oxides: a review. *Sensors* **12**, 7207–7258 (2012).
10. Weickert, J., Dunbar, R. B., Hesse, H. C., Wiedemann, W. & Schmidt-Mende, L. Nanostructured organic and hybrid solar cells. *Adv. Mater.* **23**, 1810–1828 (2011).
11. Feng, X. J., Zhu, K., Frank, A. J., Grimes, C. A. & Mallouk, T. E. Rapid charge transport in dye-sensitized solar cells made from vertically aligned single-crystal rutile TiO_2 nanowires. *Angew. Chem. Int. Ed.* **51**, 2727–2730 (2012).
12. Miao, Z. *et al.* Electrochemically induced sol-gel preparation of single-crystalline TiO_2 nanowires. *Nano Lett.* **2**, 717–720 (2002).
13. Baik, J. M. *et al.* High-yield TiO_2 nanowire synthesis and single nanowire field-effect transistor fabrication. *Appl. Phys. Lett.* **92**, 242111 (2008).
14. Shi, J. & Wang, X. D. Growth of rutile titanium dioxide nanowires by pulsed chemical vapor deposition. *Cryst. Growth Des.* **11**, 949–954 (2011).
15. Liu, B., Boercker, J. E. & Aydil, E. S. Oriented single crystalline titanium dioxide nanowires. *Nanotechnology* **19**, 505604 (2008).
16. Liao, J. Y., Lei, B. X., Chen, H. Y., Kuang, D. B. & Su, C. Y. Oriented hierarchical single crystalline anatase TiO_2 nanowire arrays on Ti-foil substrate for efficient flexible dye-sensitized solar cells. *Energy Environ. Sci.* **5**, 5750–5757 (2012).

17. Yu, X. *et al.* One-step ammonia hydrothermal synthesis of single crystal anatase TiO_2 nanowires for highly efficient dye-sensitized solar cells. *J. Mater. Chem. A* **1**, 2110–2117 (2013).
18. Liu, B. & Aydil, E. S. Growth of oriented single-crystalline rutile TiO_2 nanorods on transparent conducting substrates for dye-sensitized solar cells. *J. Am. Chem. Soc.* **131**, 3985–3990 (2009).
19. Feng, X. J. *et al.* Vertically aligned single crystal TiO_2 nanowire arrays grown directly on transparent conducting oxide coated glass: synthesis details and applications. *Nano Lett.* **8**, 3781–3786 (2008).
20. Wang, G. M. *et al.* Hydrogen-treated TiO_2 nanowire arrays for photoelectrochemical water splitting. *Nano Lett.* **11**, 3026–3033 (2011).
21. Guo, W. X. *et al.* Rectangular bunched rutile TiO_2 nanorod arrays grown on carbon fiber for dye-sensitized solar cells. *J. Am. Chem. Soc.* **134**, 4437–4441 (2012).
22. Hwang, Y. J., Hahn, C., Liu, B. & Yang, P. D. Photoelectrochemical properties of TiO_2 nanowire arrays: a study of the dependence on length and atomic layer deposition coating. *ACS Nano* **6**, 5060–5069 (2012).
23. Hoang, S., Guo, S. W., Hahn, N. T., Bard, A. J. & Mullins, C. B. Visible light driven photoelectrochemical water oxidation on nitrogen-modified TiO_2 nanowires. *Nano Lett.* **12**, 26–32 (2012).
24. Qiu, J. H. *et al.* All-solid-state hybrid solar cells based on a new organometal halideperovskite sensitizer and one-dimensional TiO_2 nanowire arrays. *Nanoscale* **5**, 3245–3248 (2013).
25. Kim, H. S. *et al.* High efficiency solid-state sensitized solar cell-based on submicrometer rutile TiO_2 nanorod and $CH_3NH_3PbI_3$ perovskite sensitizer. *Nano Lett.* **13**, 2412–2417 (2013).
26. Mahesh, S., Gopal, A., Thirumalai, R. & Ajayaghosh, A. Light-induced Ostwald ripening of organic nanodots to rods. *J. Am. Chem. Soc.* **134**, 7227–7230 (2012).
27. Liu, Y. *et al.* Substrate-free, large-scale, free-standing and two-side oriented single crystal TiO_2 nanorod array films with photocatalytic properties. *Chem. Commun.* **47**, 3790–3792 (2011).
28. Cassaignon, S., Koelsch, M. & Jolivet, J. P. From $TiCl_3$ to TiO_2 nanoparticles (anatase, brookite and rutile): Thermohydrolysis and oxidation in aqueous medium. *J. Phys. Chem. Solids.* **68**, 695–700 (2007).

Acknowledgments

This work was financially supported by the National Natural Science Foundation of China (No. 51272294), National Basic Research Program of China (No. 2012CB933704), Program for Changjiang Scholars Innovative Research Team in University (No. IRT13042), National Natural Science Foundation of China (No. 51462007), and Guangxi Natural Science Foundation (No. 2014GXNSFAA118349).

Author contributions

Y.L. and X.Y.W. proposed and designed the experiments. X.Y.W. and Y.Z. carried out the experiments and characterization. Y.L., W.H. and X.Y.W. wrote the paper. B.J.L., X.Z. and H.S. guided the work and analysis. All authors discussed the results and commented on the manuscript.

Additional information

Supplementary information accompanies this paper at http://www.nature.com/scientificreports

Competing financial interests: The authors declare no competing financial interests.

How to cite this article: Wang, X. *et al.* Confined-space synthesis of single crystal TiO_2 nanowires in atmospheric vessel at low temperature: a generalized approach. *Sci. Rep.* **5**, 8129; DOI:10.1038/srep08129 (2015).